Review

Comprehensive Review of SBA-15 Mesoporous Silica: Functionalization Strategies, Diffusion Mechanisms, and Emerging Applications

Morayma Angelica Muñoz *, Diego Robert Flores, Grace Alexandra Morillo, Ricardo Narváez, Antonio Marcilla, Marco Rosero

Posted Date: 25 September 2025

doi: 10.20944/preprints202509.2125.v1

Keywords: SBA-15; mesoporous materials; surface functionalization; diffusion mechanisms; gas adsorption; mathematical modeling

 doi:10.20944/preprints202509.2125.v1

Review

Comprehensive Review of SBA-15 Mesoporous Silica: Functionalization Strategies, Diffusion Mechanisms, and Emerging Applications

Morayma Muñoz [1,*], Diego Flores [2], Grace Morillo [3], Ricardo Narváez [2], Antonio Marcilla [1] and Marco Rosero [2]

[1] Universidad de Alicante, Chemical Engineering Department; Apartado 99, 03690 Alicante, Spain

[2] Universidad Central del Ecuador, Facultad de Ingeniería Química, UCE-GIIP

* Correspondence: moraymam@corporacionalquimia.org

Abstract

Mesoporous materials have attracted increasing attention due to their ordered pore systems, tunable surface chemistry, and versatile applications in catalysis, adsorption, and environmental technologies. Among them, SBA-15 stands out for its large surface area, uniform mesopores, and high hydrothermal stability, which make it a promising platform for gas adsorption and mass transport studies. This review examines the functionalization of SBA-15 through strategies such as post-synthesis grafting and co-condensation, focusing on the introduction of amines, thiols, and organometallic species that enhance selectivity, adsorption capacity, and thermal stability. The discussion integrates classical diffusion models, including Fickian and Knudsen transport, with more advanced approaches such as the Maxwell–Stefan formalism, to describe molecular transport within mesoporous networks and highlight the role of van der Waals interactions in gas capture processes. Special emphasis is placed on the relationship between structural features and diffusive behavior, supported by recent advances in computational modeling and spectroscopic validation. Applications in CO_2 capture, heterogeneous catalysis, drug delivery, and environmental remediation are critically assessed to illustrate the versatility of functionalized SBA-15. The review concludes by outlining future perspectives on the rational design of hierarchical and multifunctional mesoporous materials for clean energy conversion, pollutant removal, and biomedical applications.

Keywords: SBA-15; mesoporous materials; surface functionalization; diffusion mechanisms; gas adsorption; mathematical modeling

1. Introduction

Mesoporous materials are a class of hybrid inorganic or organo-inorganic solids characterized by the presence of pores in the range of 2 to 50 nanometers, according to the classification of the International Union of Pure and Applied Chemistry (IUPAC) [1]. They have emerged as versatile platforms in nanoscience due to their specific surface area (600-1500 m^2/g) depending on the synthesis method [2], typical pore volumes between 0.5 and 2.5 cm^3/g [3], morphology defined at the nanometer scale [3], and their ability to form ordered structures with uniform porosity [4].

This combination of characteristics has consolidated its relevance in applications such as heterogeneous catalysis [5], selective separation [6], and adsorption of gaseous and liquid compounds. Among them, materials such as Santa Barbara Amorphous-15 (SBA-15) have stood out for their thermal stability up to 800 °C, thicker porous walls (3.1-6.4 nm) related to materials such as MCM-41 [7,8], and the presence of interconnecting micropores that enhance molecular transport [9], which allows precise control of the porous architecture [10], controlled drug release[11], environmental remediation [12,13] and versatility to be chemically modified.

1.1. Relevance and Applications of Mesoporous Materials

 doi:10.20944/preprints202509.2125.v1

These characteristics, along with the structural tunability through synthesis parameters (surfactant type, pH, temperature, and template removal method), enable the tailoring of their physicochemical properties [4,14]. For specific application requirements, functional groups can be selectively anchored onto the surface to generate functionalized mesoporous materials.

Including specific chemical groups on the surface of the material is used for forming functionalized materials with the purpose of modifying the physicochemical properties of mesoporous materials to adapt them to requirements.

Chemical functionalization of their surfaces with groups such as amines (-NH_2), sulfhydryls (-SH), carboxyls (-COOH) and phosphonates (-PO_3H_2) has been shown to enhance the selectivity towards target molecules in adsorption and separation processes [8,9]. These groups interact by J.D van der Waals forces, hydrogen bonds or electrostatic interactions, extending their field of application towards environmental, medical and energy technologies.

Functionalized SBA-15 has shown potential in different fields such as environmental, biomedical and energy. In the environmental field, they are used in carbon dioxide capture (up to 2.5 mmol/g at 1 bar and 25 °C) and heavy metal removal, reaching efficiencies above 95 % for Pb^{2+} ions [10,12]. In the biomedical field, their compatibility and controlled porosity make them effective systems for controlled drug release, with demonstrated molecular loading efficiencies ranging from 80 to 95 % for compounds such as doxorubicin and ibuprofen [11,15]. In the energy field, mesoporous materials such as SBA-15 stand out for their thermal stability and tunable morphology, being promising for the storage of combustible gases. For example, capacities of 150 v/v have been reported for CH_4 (methane, a key vector in the energy transition) [16,17] and 2.5 wt % for H_2 (hydrogen, essential for clean energies) at 77K [20,21]. These properties make them ideal candidates for applications such as natural gas vehicle (NGV) reservoirs or hydrogen storage systems in fuel cells.

The possibility of adjusting pore size and morphology by controlling synthetic parameters such as temperature, pH, surfactant type and organic template removal methods enables to optimize the diffusion of species within the material. This aspect is necessary to maximize efficiency in dynamic processes such as gas adsorption [10,18], substrate diffusion in heterogeneous catalysis or controlled release in biomedicine [19]. Recent advances have expanded their applications towards advanced catalysis, where they function as support for metal nanoparticles (2-5 nm) with optimal dispersion that increases catalytic activity in biomass refining reactions (yields >90%) [7,20]. This multifunctionality is enhanced by the possibility of creating hierarchical structures combining micro-, meso- and macropores, optimizing molecular transport mechanisms [14,21]. The integration of organic groups into their inorganic matrix by hybrid synthesis methods has opened new routes for the development of smart materials with response to external stimuli such as pH, temperature or magnetic fields [4,22].

Regarding the environmental sector, mesoporous materials have been used in carbon dioxide capture and storage processes, volatile organic compounds (VOCs) removal, and treatment of toxic gases [8]. In medicine and biotechnology, mesoporous materials have been used as vehicles for active pharmaceutical ingredients, enabling protection and stimulus-responsive release such as pH or temperature. Their biocompatibility, structural integrity, and ease of functionalization with tissue-targeting groups make SBA-15 a promising platform for anti-tumor therapy, intelligent drug delivery systems, and advanced formulations [15].

These materials have garnered increasing research attention, with more than 15,000 publications indexed in Scopus since 2015, particularly in emerging technologies such as molecular sensors, photonics, and flexible electronics [8]. Their industrial scalability has been demonstrated in processes such as the production of heterogeneous catalysts and large-scale water purification systems [13,19,23].

2. Structural Characterization and Comparison Between Materials

These materials are characterized by a three-dimensional network of pores with controlled diameters, which endows them with unique properties. Their ordered structure results from

 doi:10.20944/preprints202509.2125.v1

cooperative self-assembly between surfactants (such as Pluronic P123) and inorganic precursors, followed by thermal or chemical removal of the organic template [24]. The structural versatility of these materials is manifested in three main configurations (Figure 1): i) hexagonal (p6mm) phases such as SBA-15 and MCM-41 with unidirectional channels, (ii) cubic (Ia3d) structures such as KIT-6 with interconnected three-dimensional porosity, and (iii) lamellar systems such as FSM-16 with two-dimensional arrangement [23,25].

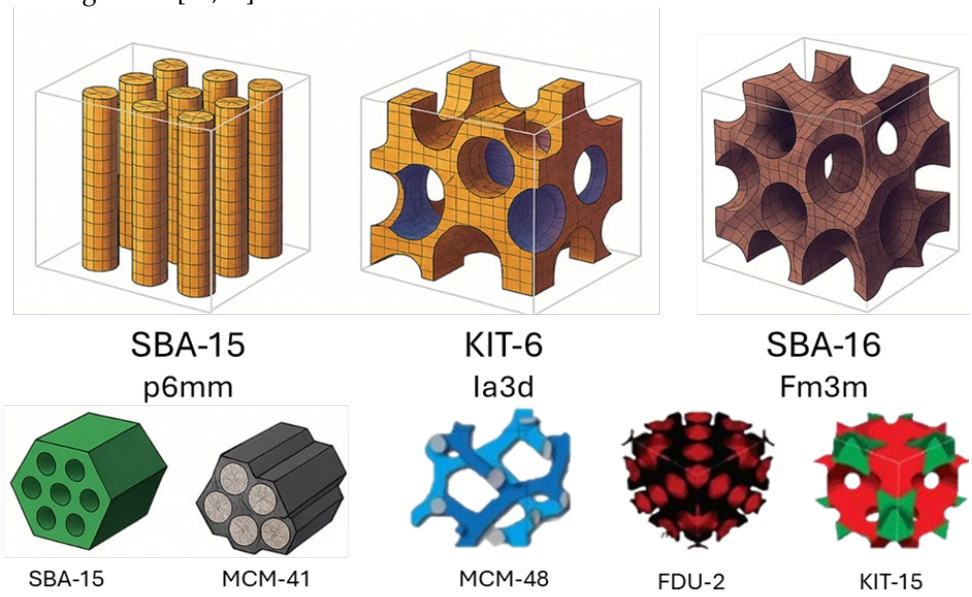

Figure 1. Schemes of ordered mesoporous structures. From left to right: SBA-15 (p6mm) with hexagonal cylindrical channels, KIT-6 (Ia3d) with interpenetrated cubic bicontinuous structure, SBA-16 (Im3m) with body-centered cubic geometry, FDU-12 (Fm3m) with open cubic.

Table 1 presents a benchmark of the most published mesoporous materials, highlighting their structural parameters and characteristic synthesis methods [24,26].

Table 1. Comparison of mesoporous materials.

Mesoporous Material	Structure	Pore size (nm)	Surface Area (m^2/g)	Typical Synthesis method	Ref.
MCM-41	Hexagonal p6mm	2–10	800–1000	CTAB-assisted sol-gel	[23,24]
SBA-15	Hexagonal p6mm	5–30	500–1000	P123-templated sol-gel	[20,24]
KIT-6	Cubic Ia3d	6–12	400–900	P123/butanol cosurfactant system	[26,27]
FDU-12	Cubic Fm3m	5–15	600–900	Modified triblock copolymers	[26,28]
MSU-X	Disordered	2–12	500–700	Nonionic self-assembly	[27]
TUD-1	Interconnected	3–10	600–850	Surfactant-assisted sol-gel	[27]
MCM-48	Cubic Ia3d	2–4	800–1100	CTAB-templated sol-gel	[23,24]
FSM-16	Lamellar	2–3	900–1000	Surfactant intercalation	[23]

Control over the synthesis of materials allows to design mesostructures with different orientations, connectivities and surface morphologies, which significantly influences the efficiency of adsorption, encapsulation or catalysis processes. In this sense, mesoporous materials act as a structural interface between microporous zeolites (<2 nm) and macroporous materials (>50 nm), offering accessible, functionalizable and thermally stable surfaces. [29]

 doi:10.20944/preprints202509.2125.v1

Structural characterization is essential to correlate the physicochemical properties of the material with its functional performance. Key parameters such as surface area (600-1200 m^2/g), pore volume, and wall thickness are strongly dependent on the type of surfactant, acidity of the medium, water/precursor ratio and thermal aging conditions [29,30]. Modification of these parameters favors accessibility to active sites, increases catalytic efficiency and improves host-guest interaction. A larger surface area facilitates the modification of surface or molecular charge [23,24]. In particular, SBA-15 presents secondary micropores (0.5-2 nm) connected to the main mesoporous channels, which increases the accessibility to active sites (>90 %) and improves molecular diffusion. For the case of CO_2, with reported effective diffusivities D_{eff} on the order of $10^{-7}\ m^2/s$, outperforming non-hierarchical analogues of similar composition [29].

The surface properties of mesoporous materials can be modulated by chemical modification through the targeted inclusion of functional groups such as amino (-NH_2), thiol (-SH), carboxyl (-COOH) or sulfonate (-SO_3H). These groups enable specific interactions with gases, metal ions or biomolecules by electrostatic interactions or J.D van der Waals forces [15,19]. The introduction of amino groups increases the adsorption capacity of CO_2 up to 2.8 mmol/g (1 bar, 25°C), 150 % higher than non-functionalized materials. However, the heterogeneous distribution of active sites in pores <4 nm remains a challenge for large-scale applications [31]. On the other hand, adding noble metals such as Pt or Pd by impregnation methods generates catalytic centers with high surface dispersion (around 80 %), improving the activity in hydrogenation or selective oxidation reactions. Mesoporous materials can be composed of pure silica as in the case of SBA-15, or incorporate heteroelements such as Al, Ti, Fe or Zr by direct synthesis or post-synthesis modification, this change in composition affects the acid-base, redox properties and thermal stability [23].

The hydrophilicity of mesoporous materials is primarily determined by the density of surface silanol groups and by the heat treatment applied during or after synthesis. This property can be tuned by functionalization with organosilanes, addition of additional silanols, or plasma treatments, to enhance compatibility with aqueous or biological media. Controlling hydrophilicity is particularly relevant in controlled drug release or the design of chemical sensors [15,30]. The surface activity of mesopores is determined by the functional groups available after synthesis or modified subsequently.

In addition to hydrophilicity, pore geometry is another critical factor determining the efficiency of these materials. The geometry of SBA-15 favors adsorption and catalysis processes requiring unidirectional molecular transport, whereas the cubic structure of KIT-6 is used for reactions demanding multidirectional diffusion [23,24]. Recent advances have demonstrated that precise control of secondary microporosity and surface functionalization allows the design of materials with tailored properties [3], [15,21,29,30].

2.1. Structure and Synthesis of SBA-15

Ordered mesoporous materials such as SBA (Santa Barbara Amorphous) are versatile platforms in materials science. In particular, SBA-15, developed by Zhao in 1998, features a structure of hexagonally ordered cylindrical pores (space group p6mm) interconnected by micropores in the walls, facilitating molecular transport [7,14]. It typically exhibits pore diameters in the range of 5–30 nm, thick walls (~3–6 nm), a high specific surface area (600–1000 m^2/g), and a pore volume reaching up to 1.5 cm^3/g. [18,24]

SBA-15 consists of a pure amorphous SiO_2 matrix, whose three-dimensional organization is induced by the micellar self-assembly of the surfactant P123 ($EO_{20}PO_{70}EO_{20}$) [18,24], which acts as a structural template in acidic medium. Under these conditions, PPO chains of P123 become hydrophobic while PEO chains remain hydrated, leading to the formation of cylindrical micelles. Silica precursors as tetraethyl orthosilicate (TEOS) or Na_2SiO_3, hydrolyze and condense around the micelles through $S^0H^+X^-I^+$ electrostatic interactions (S^0 = P123, X^- = Cl^-, I^+ = silica species) [18]. A thermal aging step at 100–130 °C enhances the ordering and wall thickness (3–6 nm) [14,26]. Calcination at 500–550 °C then removes the template, leaving a thermally stable mesoporous structure up to 800 °C.

 doi:10.20944/preprints202509.2125.v1

In addition to P123, the chemistry of the system can be modified by introducing co-surfactants (CTAB), adjusting the pH, temperature, or type of silica precursor, which allows modulation of the morphology, porosity, and connectivity of the final solid. Such synthetic control enables the tailoring of SBA-15 to be tailored for specific applications requiring efficient molecular transport or advanced functional selectivity.

2.2. Synthesis Methods and Their Effect on Diffusive Properties

The synthesis of SBA-15 can be tailored by a variety of techniques, from conventional methods such as sol-gel to microwave-, ultrasound- or solvothermal-assisted processes. Each variant modifies the textural properties of the material, especially the pore size, wall thickness and crystallinity of the siliceous phase, which directly affects its efficiency in mass transport processes. Table 2 summarizes the main synthesis methods, operating conditions, and associated advantages.

Table 2. SBA-15 synthesis methods and their characteristics

Synthesis method	Conditions	Pore size (nm)	Deff (m^2/s)	Key Advantages	Ref.
Conventional sol-gel	HCl, 35–40 °C, 24–72 h	6–8	~1.0×10^{-8}	High ordering, easy scalability	[18]
Hydrothermal	100–130 °C, 24–48 h	6–10	1.2×10^{-8}	Enhanced crystallinity, structural stability	[7,26]
Microwave-assisted	2.45 GHz, 80–100 °C, 1–2 h	5–8	3.5×10^{-7}	Rapid synthesis, uniform particle size control	[3,28]
Sonochemical	Ultrasonic frequency, low T	5–9	1.5×10^{-7}	Improved homogeneity, morphological dispersion	[21]
Solvothermal	Organic solvents, high pressure	5–7	~1.8×10^{-8}	Precise shape/crystallinity/particle size control	[23]
Dual-template (P123/CTAB)	Mixed surfactants	4–12 (bimodal)	~1.0×10^{-8}	Hierarchical meso-macroporous structures	[9]
Post-synthesis grafting	Grafting con –NH_2, tioles, etc.	4–7	2.8×10^{-7}	Tailored surfaces for selective adsorption/catalysis	[10,16]

3. Functionalization of Mesoporous Materials: Strategies, Properties

Modifying mesoporous materials represents a paradigm shift in the design of solids with tailored surface chemistry and diffusion behavior at the nanoscale [32,33]. This section critically analyzes the functionalization strategies, their impact on physicochemical properties, and the structure-activity correlations in gaseous fluids.

Materials such as SBA-15, MCM-41 and KIT-6 have proven to be versatile platforms due to their high surface area, structural ordering and possibility of chemical modification through covalent grafting techniques, co-condensation or incorporation of metallic and supramolecular species [10,34,35], as well as hybrid structures such as mesoporous carbons, MOFs, and silicas doped with heteroelements. These modifications enable precise tuning of host–guest interactions and the regulation of mass transport mechanisms according to system-specific requirements.

While the discussion here focuses on SBA-15 due to its widespread use as a model material, the described strategies are equally applicable to other mesoporous silica-based materials such as MCM-41, KIT-6, or disordered systems like MSU-X [4,24,36]. The choice of method critically depends on: (i) the active site density, (ii) the pore accessibility, and (iii) the thermal and chemical stability of the resulting material [36]. The main strategies for the modification of mesoporous silicas such as SBA-15 and their impact on textural and functional properties are described below.

Post-synthesis grafting is a two-step method that involves the covalent attachment of organosilanes such as 3-aminopropyl)triethoxysilane (APTES) to surface silanol groups under strict

 doi:10.20944/preprints202509.2125.v1

anhydrous conditions (reflux in toluene at 110°C under a N_2 atmosphere). The reaction proceeds by nucleophilic substitution: $\equiv Si - OH + (EtO)_3Si - R \rightarrow Si - O - SI - R + 3EtOH$.

This procedure preserves the hexagonal structure and enables control over the functional group density (0.5–3.0 groups/nm²), although it t typically leads to a ~25% reduction in pore diameter and surface area and limited thermal stability (~250 °C) due to bond degradation [16,37]. However, it can present heterogeneous distribution in narrow pores (<4 nm) and limits its thermal stability (~250°C) without altering the porous architecture of SBA-15 [34,38]. This method is suitable for situations requiring controlled surface modifications, such as CO_2 capture.

An effective alternative is direct co-condensation, where functional precursors are simultaneously incorporated with TEOS and functional silanes such as 3-mercaptopropyltrimethoxysilane (MPTMS) in the presence of the Pluronic® P123 surfactant during the synthesis of the mesoporous material. This method has demonstrated a more homogeneous integration of active groups such as –SH or $–NH_2$ (approximately 1.2–3.5 groups/nm²) within the silica backbone, although it typically results in a pore size reduction of approximately 25% of the BET area (1–2 nm) and presents lower thermal stability (<200°C) [10,24,36].

Methods such as impregnation with metal nitrates (Cu^{2+}, Fe^{3+}, Ni^{2+}) and subsequent calcination generate active sites that allow efficient catalytic processes, such as CH_4 oxidation or Fenton-type reactions, achieving conversion rates exceeding 90% in systems such as Cu/SBA-15 [39–41]. Additionally, the isomorphic substitution of Si^{4+} by Al^{3+} in the network generates Brønsted acid sites without compromising the integrity of the SBA-15 framework, improving its activity in acid catalysis and selective adsorption processes [17,42]. This method does not significantly alter the Brunauer Emmett Teller (BET) area (–10%) and offers thermal stability (~600°C) [43], ideal for catalytic systems that require noble metals (Pt, Pd) under severe conditions.

More recently, modification through supramolecular interactions has gained relevance, where the density of groups varies depending on the host, but reduces the BET area by 20% and has low thermal stability (<200°C) [3]. This allows adding guest molecules such as β-cyclodextrin (β-CD), capable of forming inclusion complexes with organic contaminants, heavy metals or pesticides. Hybrid systems such as SBA-15 functionalized with β-CD have been shown to improve adsorption, as is the case with methylene blue where it reached up to 1791 (mg/g), thanks to host–guest interactions and electrostatic bonds between amino groups and sulfonated groups, through amide linkages or covalent grafting, which improves the removal of metal ions such as Cd^{2+}, Hg^{2+} or Pb^{2+}, with efficiencies greater than 90% [35]. Furthermore, their inclusion in hybrid structures such as MOFs or PVDF membranes allow adsorbents to be recovered for up to five cycles with minimal capacity loss [34,35].

Emerging methods, such as the anchoring of β-cyclodextrin or azobenzene onto the surface of SBA-15 through photoactive modification, allow creating materials capable of responding to external stimuli such as light, pH, or redox conditions. These materials exhibit advanced properties such as high CO_2/N_2 selectivity (>200) or photoactivated diffusion control [3,38]. Therefore, they are used in the selective adsorption of pollutants through host–guest interactions.

Functionalization typically induces changes in textural properties, including a decrease in BET surface area and pore size; however, these effects are often offset by improved adsorption capacity, selectivity, and surface reactivity [17,34]. SBA-15 modified with β-CD and amines showed synergy in the capture of aromatic pollutants, validated both experimentally and through DFT calculations and two-dimensional nuclear magnetic resonance (NMR) spectroscopy [34].

The field of mesoporous materials has evolved toward a diversification in both the base structures and the functional groups introduced. This versatility has enabled applications across new areas, such as fine catalysis, selective environmental remediation, magnetic separation, and targeted drug release.

Figure 2 summarizes the main functionalization strategies reported for SBA-15, including 3-aminopropyl)triethoxysilane (APTES) based amination, post-synthesis oxidation to introduce

Preprints.org (www.preprints.org) | NOT PEER-REVIEWED | Posted: 25 September 2025 doi:10.20944/preprints202509.2125.v1

carboxyl groups, metal impregnation (Pt, Pd), Schiff-base formation for heavy metal capture, and the inclusion of magnetic nanoparticles such as Fe_3O_4.

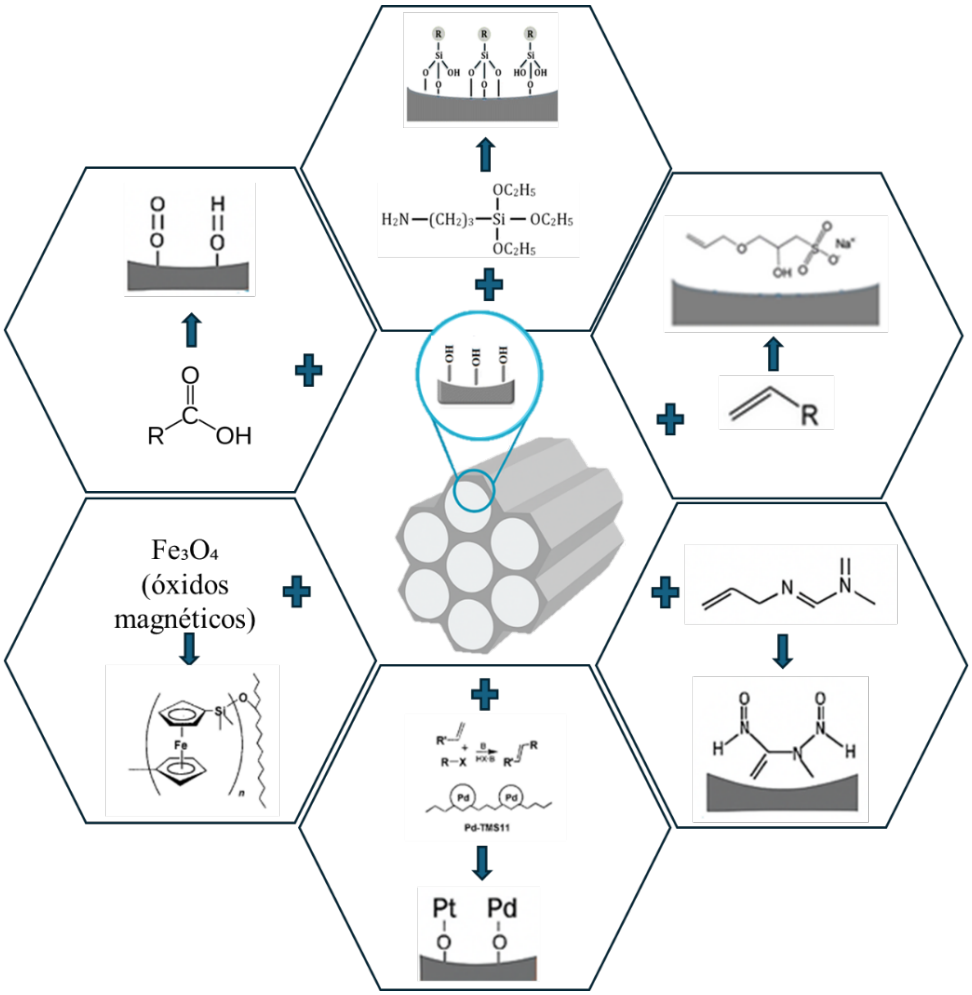

Figure 2. Representative diagram of the functionalization routes for SBA-15 with different active groups. Strategies such as APTES grafting (amino groups), post-synthesis oxidation to introduce carboxyl groups, incorporation of magnetic oxides (Fe_3O_4), formation of Schiff-base structures, and inclusion of organic groups (alkyls, phenyls) are illustrated.

Table 3 compiles representative examples of functionalized mesoporous systems, detailing support structures, chemical modifications, synthetic approaches, processing conditions, and primary applications. Highlighting not only the support structure (SBA-15, MCM-41, KIT-6, CMK-3, MOFs), but also the type of chemical modification, the synthetic method used, typical operating conditions, and the associated main application. Functionalized SBA-15 consistently demonstrates enhanced CO_2 adsorption capacities ($q_{a5s} \geq 2.8$ mmol/g at 1 bar, 25°C) and improved acid catalysis performance (TOF: 15–40 h^{-1}) compared to non-functionalized analogues [38,44].

This summary highlights the critical role of rational support–modifier pairing and incorporation protocols in determining material efficiency, while also reflecting a clear trend toward multifunctional and hybrid materials with enhanced reusability and structural integrity under demanding conditions.

 doi:10.20944/preprints202509.2125.v1

Table 3. Functionalized mesoporous materials: methods and conditions

Base Material	Functional Group / Modifier	Incorporation Method	Conditions	Application	Ref.
SBA-15	–NH_2 (aminopropyl, APTES)	Grafting	EtOH, 60–80 °C, 12–24 h	CO_2 capture, drug immobilization, VOCs	[10,37,45,46]
SBA-15	Bis-Schiff base	3-step anchoring (silanization + condensation)	Organic solvent, RT–80 °C	Selective removal of Pb(II) and other metals	[12,33]
SBA-15	–COOH (carboxylic acid)	Post-synthesis oxidation	HNO_3, 50–80 °C, 6–12 h	Adsorption of dyes, metals	[15,43]
SBA-15	–SH (thiol)	Co-condensation or grafting	pH acid, 25–50 °C	Adsorption of noble metals (Au, Ag, Pt)	[15,43]
SBA-15	Fe_3O_4 (magnetic oxides)	Coprecipitation in mesostructure	60–90 °C, pH 8–9	Magnetic separation, reuse	[15,39]
SBA-15	Pt/Pd o Ni, Cu	Impregnation + reduction	200–300 °C, H_2 o Ar	Heterogeneous catalysis (hydrogenation, oxidation)	[33], [40,42,47,48]
SBA-15	Organic groups (alkyls, phenyls)	Grafting or co-condensation	RT–120 °C, organic solvent	Hydrophobicity tuning, drug anchoring	[11,49]
SBA-15	β- Cyclodextrin (β-CD)	Modification by supramolecular anchoring	RT–50 °C, aqueous solvent	Adsorption of organic contaminants	[34,35]
SBA-15	Azobenzene	Photoactive modification	RT–60°C Organic solvent UV (365 nm) or visible (>450 nm) light	Photoactivated diffusion control, sensors	[3,38]
MCM-41	–COOH (carboxylic acid	Post-synthesis oxidation	APS, HNO_3, 50–80 °C	Adsorption of dyes	[43]
KIT-6	–SH (thiol)	Co-condensation	pH acid, 25–50 °C	Adsorption of heavy metals (Hg^{2+}, Cd^{2+})	[15]
CMK-3	–SO_3H (sulfonic acid)	Reflux with H_2SO_4	80–120 °C, 6–12 h	Esterification, acid catalysis	[32]
MOF-5	–NH_2, –COOH	Reflux with H_2SO_4	Solvothermal tempering	Selective adsorption, sensors, catalysis	[4]

The choice of functional group depends on the application objective. Amino groups (-NH_2) favor interactions with anionic species, heavy metals and allow the immobilization of biomolecules [12,15]. Thiol groups (-SH) have an affinity for noble metals (Au, Ag, Pt) and are used in catalysis and selective detection [15,43]. Phosphonic groups (-PO_3H_2): Improve thermal stability and introduce acid sites for acid catalysis [3,50]. And organic functional groups (phenyls, alkyls, carboxyls) adjust hydrophobicity, polarity and allow the anchoring of specific drugs or catalysts [11,49]. These routes allow the SBA-15 to surface to be tailored for specific applications such as metal capture, selective adsorption and targeted drug release [6,17,51].

 doi:10.20944/preprints202509.2125.v1

4. Diffusion Mechanism of Substances in Mesopores: General Model Applied to SBA-15

Mass transport in ordered mesoporous materials is governed by a complex interplay of pore geometry, surface interactions, and multiple concurrent diffusion mechanisms operating under various thermodynamic conditions. This process involves coupled mechanisms of volumetric diffusion, surface diffusion, and adsorption-desorption phenomena operating at multiple spatial and temporal scales. Understanding these transport mechanisms is crucial for optimizing material performance [11,52,53].

Mathematical modeling of transport in these media is generally approached using continuous approximations based on partial differential equations (PDEs), considering pore geometry, local crystal structure, surface heterogeneity, and molecular migration and retention mechanisms. These models allow estimating operating parameters such as the effective diffusion coefficient, adsorption rate, and concentration profile, which are difficult to measure directly in complex porous media [54]. Molecular transport in SBA-15 is commonly modeled by partial differential equations that describe the temporal and spatial evolution of solute concentration [55,56].

4.1. Modeling Diffusion and Transport Mechanisms.

Mass transport in ordered mesoporous materials, such as SBA-15, is a multifactorial process involving complex interactions between pore geometry, surface roughness, chemical functionalization, and the surrounding thermodynamic conditions. This behavior involves coupled volumetric and surface diffusion along with reversible adsorption phenomena, which operate at multiple spatial and temporal scales [54].

Under ideal conditions (isothermal regime (298–323 K), low pressure (P < 1 atm), and absence of convective flow), mass transport can be adequately described by Fick's law (Eq. 1). This is valid when internal surfaces do not present active functionalization, and homogeneous concentration gradients are maintained [30]. Under these conditions, diffusion predominantly proceeds via molecular mechanisms, which allows the use of simplified one-dimensional models to estimate the effective diffusion coefficient within the mesoporous framework [52,56]. However, characterization studies using experimental techniques (NMR, X-ray scattering) and molecular simulations [57] have reported cases of anomalous or non-Fickian diffusion when the mesoporous material presents complex microstructures, irregular connectivities or molecular confinement, interfacial forces [58]. This behavior is often attributed to factors such as: (i) irregular micropore connectivity, which induces tortuous paths and prolonged molecular residence times, and (ii) confinement effects in sub-10 nm pores, where wall collisions dominate over intermolecular collisions, favoring Knudsen-type transport. Molecular confinement in pores <10 nm, molecule-wall collisions dominate over intermolecular collisions, activating Knudsen mechanisms [59].

SBA-15 not only possesses primary mesopores, but also micropores within the walls that interconnect the main channels. The presence and relative proportion of these micropores can change the dominant mechanism: from a zeolitic-type diffusion in micropores to a faster one in secondary mesopores [60]. Moreover, the interaction energy between adsorbate and surface significantly influences local concentration gradients and overall transport dynamics [61].

The introduction of functional groups significantly alters the mass transport mechanisms in mesoporous materials. Functionalization can either enhance diffusion or promote selective sorption, depending on the nature of the chemical group and the type of interaction with the sorbate. Adding functional groups into SBA-15 modifies the energy interaction between sorbate molecules and pore walls, thereby influencing diffusion mechanisms [20]. For instance, amine groups (–NH_2) increase the adsorption energy of CO_2 via carbamate formation (E_{ads} ≈ 50–80 kJ/mol), which reduces the effective diffusivity (D_{eff}) while enhancing adsorption capacity [16]. Thiol groups (–SH) promote heavy metal (Pb^{2+}) adsorption, with surface diffusion coefficients (D_s) governed by a thermally activated hopping

 doi:10.20944/preprints202509.2125.v1

model [35]. Sulfonate groups (–SO_3H), on the other hand, introduce surface charges that modulate ionic diffusion through electrostatic interactions [12].

4.1.1. Molecular Diffusion (Fickian)

In pores larger than 10 nm and under low-pressure conditions (P < 1 atm), mass transport follows Fick's law, which predominates when the pore diameter (d_p) is significantly greater than the molecular mean free path (λ) for $\lambda \gg d_p$ (pore diameter between 0.5 and 2 nm versus pores of 5 to 10 nm). In this regime, collisions between diffusing molecules are dominant over interactions with the pore walls, and the mass flux is described by:

$$\vec{j} = -D_m \nabla C \quad (1)$$

When modeling transport within a cylindrical pore such as the pure SBA-15 channels (with pores >10 nm and at moderate pressures), the diffusion equation must be formulated in cylindrical coordinates $(r, \emptyset, z)$. In cases with axial symmetry and no angular or axial dependence, the one-dimensional Fick is [52,56]:

Volumetric transport equation [62]:

$$\frac{\partial C(r,t)}{dt} = D_{eff}\left(\frac{\partial^2 C}{\partial r^2} + \frac{1}{r}\frac{\partial C}{\partial r}\right) \quad (2)$$

4.1.2. Knudsen Diffusion

When the mean free path is comparable to or greater than the pore diameter is $\lambda \geq d_p$. E In this regime, collisions between molecules are rare and most collisions occur against the channel wall, generating more restricted transport [59]. This regime is relevant for CO_2 capture at low pressures [20]. The Knudsen coefficient D_k is defined as:

$$D_k = \frac{d_p}{3}\sqrt{\frac{8RT}{\pi M}} \quad (3)$$

4.1.3. Combined Diffusion: Bosanquet Model

When both regimes coexist, which is common in functionalized SBA-15 operating at ambient conditions, the transport can be described by a Bosanquet resistance model (4). Transport in the channel volume is dominated by two mechanisms acting in parallel: Knudsen diffusion (D_k) and free-phase molecular diffusion (D_m) [62]. The overall effective diffusion coefficient (D_v) is described as:

$$D_v = \left(\frac{1}{D_k} + \frac{1}{D_m}\right)^{-1} \quad (4)$$

Molecular diffusion:

$$D_m = \frac{1}{3}\lambda\bar{v}, \qquad \bar{v} = \sqrt{\frac{8RT}{\pi M}} \quad (5)$$

4.1.4. Surface Diffusion

Surface diffusion occurs when adsorbed molecules migrate laterally between active sites along the internal pore surface, typically via van der Waals or hydrogen bonding. [63].

$$D_s = \Gamma a^2 e^{\left(-\frac{E_a}{RT}\right)} \quad (6)$$

This mechanism is particularly relevant in SBA-15 functionalized with –NH_2, –SH or transition metal groups [3,46].

 doi:10.20944/preprints202509.2125.v1

4.1.5. Multicomponent Diffusion: Maxwell–Stefan Model

In multicomponent systems, Fick's law is often insufficient due to the presence of molecular interactions. Instead, the Maxwell–Stefan framework accounts for these interactions via chemical potential gradients [34,52,64]:

$$-\frac{q_i}{RT}\nabla\mu_i = \sum_{j\neq i}\frac{\theta_j j_i - \theta_i j_j}{D_{ij}} + \frac{j_i}{D_{oi}} \quad (7)$$

In the case of CO_2 capture in SBA-15 functionalized with amino groups (-NH_2), it has been shown that the formation of carbamates modifies the transport mechanism, reducing the effective diffusivity due to chemical retention processes at the surface. Therefore, the Maxwell-Stefan model (Eq. 7) generalizes transport by considering chemical potential gradients and intermolecular interactions (D_{ij}). According to Kärger and Ruthven, the D_{ij} coefficients can be estimated using the Vignes correlation (Eq. 8), linking the diffusivities of pure components [52]. This correlation predicts a decrease in D_{eff} due to the formation of stable surface complexes such as carbamates, consistent with experimental findings [51].

In complex porous systems such as functionalized SBA-15, molecular transport is governed by multiple mechanisms operating at distinct spatial scales. To describe this behavior, models that consider both molecular interactions and the structural constraints of the material are combined. Two key equations are the Vignes correlation and the coupling model for hierarchical systems (systems that combine multi-scale pores micro- <2 nm, meso- 2–50 nm, and macropores >50 nm into a controlled architecture [17]):

Vignes correlation [64,65]:

$$\frac{1}{D} = \frac{1}{D_{oi}} + \frac{1}{D_{ij}} \quad (8)$$

Coupling model for hierarchical systems (Equation 9) where global transport integrates interfacial barriers [52].

$$\frac{1}{D_{global}} = \frac{1}{D_{micro}} + \frac{1}{\alpha l} \quad (9)$$

In the simple case of equally spaced transport resistances (the spacing l is assumed to be small compared to the particle length L) and permeability equal to α, in SBA-15 with interconnecting micropores, Dmicro limits overall transport if αl is large (accessible principal pores) [55].

These transport equations are conceptually analogous to electrical resistance in series, where the inverse of the diffusivity (1/D) represents a diffusive resistance. Equation 8 considers competitive resistances between molecules, while equation 9 integrates scalar resistances (micro → macro), while the hierarchical model requires porometric characterization (N_2 adsorption) to determine l and α [55].

4.1.6. Adsorption–Desorption: Kinetic Mechanism

The presence of functional groups on the walls of SBA-15 introduces nonlinear behavior into the transport dynamics due to reversible adsorption and desorption processes. The kinetics of reversible adsorption/desorption at the surface are described by the following rate expressions:

$$\text{Adsorption:}\quad r_a = k_a C_v(1-\theta) \quad (10)$$

$$\text{Desorption:}\quad r_d = k_d\theta \quad (11)$$

A two-phase model couples pore volume diffusion in the pore volume ($\vec{J}$), surface adsorption (r_a) and desorción (r_d) kinetics as follows:

$$\frac{\partial C_v}{dt} = \underbrace{D_v\nabla^2 C_v - k_a C_v}_{r_a}\underbrace{(1-\theta)}_{r_d} + k_d\theta \quad (12)$$

 doi:10.20944/preprints202509.2125.v1

$$\frac{\partial \theta}{dt} = \underbrace{D_s \nabla^2 \theta - k_a C_v}_{r_a} \underbrace{(1-\theta)}_{r_d} + k_d \theta \quad (13)$$

One application of the two-phase model is the design of adsorbents for CO_2 capture under post-combustion conditions [16,17]. For APTES-functionalized SBA-15, the equations predict the volumetric CO_2 concentration (C_v), to decay exponentially along the pore according to $\nabla^2 C_v \approx k_a C_v / D_v$ (adsorption-controlled domain), while the surface coverage (θ) reaches 80% in less than 10 seconds at 50 °C, according to in situ FTIR spectroscopy data The combination of high mesopore transport rates $D_v \sim 10^{-7} m^2/s$ and irreversible adsorption kinetics ($k_d \sim 10^{-5} s^{-1}$) accounts for the high CO_2 capture capacity (2.8 mmol/g at 1 bar) observed in APTES-functionalized SBA-15 [10]. These results, supported by in situ FTIR spectroscopy, demonstrate how coupled equations for Cv and θ enable performance predictions under real-world conditions, such as in post-combustion capture or purification systems [10,17,45].

Contribution of Nonpolar van der Waals Forces

In functionalized mesoporous materials, both physical and chemical adsorption mechanisms may coexist, depending on the nature of the adsorbate. This duality has been well documented, particularly in CO_2 adsorption on SBA-15–NH_2, where chemisorption dominates. The increased residence time of molecules on the functionalized surface results in a reduced effective diffusion coefficient D_{eff}. [20,49,63]

In contrast, the adsorption of nonpolar gases such as N_2 and CH_4 is primarily governed by van der Waals forces. These interactions are physical in nature and depend on the polarizability of the molecules and the adsorbate–adsorbent distance.

Thus, incorporating van der Waals interactions is essential in diffusion models, particularly for systems involving apolar gases and where no chemical bonding occurs. Although these interactions are weaker than covalent or ionic bonds, they can dominate adsorption behavior under ideal conditions, significantly affecting gas separation or volatile compound storage processes. These interactions, although weaker than chemical ones, can dominate adsorption behavior under ideal conditions, when working with apolar gases. Their correct inclusion in the models allows to improve the predictability of diffusion and to adjust the design of materials for specific processes such as gas separation or storage of volatile compounds. Equation 14 provides a simplified representation of the Lennard-Jones potential [54,57,66], which describes non-covalent interactions between neutral molecules. In this model, the adsorption energy (E_a) is directly proportional to the van der Waals interaction constant and inversely proportional to the sixth power of the intermolecular distance (l_{pp}).

$$E_{ads} \propto \frac{A}{{l_{pp}}^6} \quad (14)$$

This modeling approach is applicable to the design of adsorbents, heterogeneous catalysts, and controlled release systems, where the prediction of weak adsorption phenomena is essential.

5. Challenges and Future Perspectives

Mesoporous materials such as SBA-15 have proven effective in catalysis, gas separation, energy storage, and controlled drug delivery. Nonetheless, their development faces several challenges, particularly in engineering hierarchical pore architectures (micro–mesoporous, branched, or spherical morphologies) that enhance mass transport and active site accessibility. Achieving such architecture typically requires stringent synthesis conditions, including precise control of pH, temperature, and surfactant concentration. Similarly, functionalization with specific groups requires additional synthesis steps and costly reagents, which may hinder scalability [67,68].

In the energy sector, mesoporous materials are being actively explored as components in solar cells, batteries, thermoelectric devices, and photocatalysts. According [69], mesoporosity plays a

 doi:10.20944/preprints202509.2125.v1

critical role in clean energy technologies by enhancing active phase dispersion and increasing surface area, thereby improving energy conversion efficiency.

In environmental catalysis, functionalized SBA-15 has shown efficacy in removing heavy metals and organic pollutants. The functionalization of SBA-15 surfaces has been shown to improve selectivity toward specific analytes in environmental applications [68].

Furthermore, emerging biomedical applications represent an interesting frontier for mesoporous structures. The potential of SBA-15 and its functionalized derivatives for drug delivery, optical sensing, and bone regeneration scaffolds have been demonstrated, owing to their biocompatibility and ordered mesostructure [21].

Future developments are expected to focus on the hybridization of SBA-15 with active phases such as metal nanoparticles, conductive polymers, or photocatalysts. These hybrid materials aim to address current challenges in energy storage, contaminant detection, and selective gas adsorption [68,69].

A significant limitation is the heterogeneous distribution of functional groups resulting from post-synthesis grafting, which compromises reproducibility and reduces transport efficiency, especially in narrow pores (<4 nm). Additionally, functionalized materials may suffer from reduced stability due to thermally or chemically labile surface bonds [68].

Regarding mass transport modeling, Classical models such as Fick or Knudsen are often insufficient to describe mass transport in functionalized mesoporous materials, as they do not account for sorbate–sorbent interactions or multicomponent effects. The Maxwell–Stefan approach provides a more realistic framework but presents practical challenges due to the difficulty of determining key parameters such as: The cross-diffusion coefficient (D_{ij}), of the interactions between adsorbed species (CO_2/NH_3 in SBA-15-NH_2) that require complex experimental data from in situ spectroscopy [52]. The adsorption energies (E_{ads}): Vary depending on the functional groups (-NH_2 vs -SO_3H) and the heterogeneous distribution of active sites [16,37], and the surface coverage fraction (θ): Depends on the density of functional groups and residual humidity, difficult to measure in nanometric pores [31].

Experimental validation of diffusion models remains challenging, primarily due to the difficulty of directly measuring effective diffusivities. These parameters are essential for predicting selectivity in gas separations and kinetics in drug release applications. However, accurate quantification often requires advanced techniques such as Pulsed Field Gradient Nuclear Magnetic Resonance (PFG-NMR) or Quartz Crystal Microbalance with Dissipation monitoring (QCM-D), which, despite their value, are limited by cost and availability [31].

6. Conclusions

SBA-15 mesoporous silica represents a highly versatile and tunable platform with diverse applications in catalysis, gas separation, chemical sensing, and biomedicine. Its well-ordered mesostructure, high surface area (>500 m^2/g), and controllable pore size (5-30 nm) make it particularly suitable for processes where mass transport is critical. However, alternative mesoporous materials such as KIT-6 (3D cubic structure) and MCM-41 (smaller 2-4 nm pores) offer complementary advantages depending on specific application requirements. While these systems share common functionalization approaches (grafting, co-condensation), material selection should be guided by key parameters including diffusion pathway geometry (unidirectional versus three-dimensional transport), molecular dimensions of target species, and required thermal/chemical stability thresholds.

Strategic surface functionalization of SBA-15 with chemical moieties such as amine, thiol, sulfonate, or organometallic groups has significantly enhanced its selectivity and adsorption capacity for target species such as CO_2, heavy metal ions, and persistent organic pollutants. Nevertheless, several technological challenges remain, including: (1) non-uniform distribution of active sites, (2) susceptibility to degradation under extreme pH or thermal condition, and (3) difficulty in preserving structural integrity in heavily modified or hybrid configurations. Overcoming these limitations will

 doi:10.20944/preprints202509.2125.v1

require advanced synthesis protocols and robust characterization techniques to unlock the full potential of functionalized mesoporous systems.

While classical transport models (Fick's Law, Knudsen diffusion) remain useful for simplified systems, they often fail to capture the nonlinear sorbate–sorbent interactions and multicomponent effects present in functionalized structures. More sophisticated approaches such as the Maxwell–Stefan model offer a rigorous alternative, yet their implementation is constrained by the need for detailed input parameters (cross-diffusivities, adsorption energies), which are difficult to obtain experimentally.

Future advances are expected in the development of hierarchical mesoporous materials through the addition of hybrid phases such as metallic nanoparticles or conductive polymers and multiscale computational methods with experimental validation. These approaches will allow the design of functional supports with tailored properties. These innovations aim to overcome the limitations of single-porosity systems by integrating macropores for enhanced molecular transport, mesopores for high adsorption capacity, and micropores for improved selectivity.

Finally, the integration of SBA-15-based materials into practical systems—such as adsorption beds, membranes, or microfluidic platforms—represents a critical step toward their scalable and sustainable industrial deployment.

7. Further Steps

Ongoing research on functionalized mesoporous materials like SBA-15 is paving the way for a new generation of hierarchical hybrid architectures capable of integrating multiple functionalities within a single platform. By engineering synergistic micro-mesoporous networks with precisely controlled geometries (spherical, lamellar, branched), researchers aim to optimize adsorption efficiency and active site accessibility under real operating conditions. Particularly promising is the strategic incorporation of embedded functional phases, such as metallic nanoparticles, stimuli-responsive polymers, MOF structures, and biofunctional matrices, to tailor materials for specific applications.

Future breakthroughs are anticipated in the development of advanced mathematical models to describe diffusion and reaction phenomena in mesoporous systems. The integration of artificial intelligence (AI) and machine learning (ML) is expected to transform predictive modeling, particularly in combination with multiscale Maxwell–Stefan formulations that include adsorption–desorption kinetics. These models will be validated through state-of-the-art techniques such as PFG-NMR and QENS, enabling precise in situ characterization of transport dynamics.

This combined computational-experimental approach will drive the rational design of next-generation functionalized materials for critical applications. Key focus areas include selective separation processes for valuable compounds (CO_2 capture, rare-earth element recovery), targeted delivery systems with stimuli-responsive release mechanisms, and high-density storage solutions for energy carriers (H_2, CH_4) under extreme environmental conditions. The goal is to develop smart, multifunctional materials that push the boundaries of what's possible in fields ranging from sustainable energy to precision medicine.

Abbreviations

The following abbreviations are used in this manuscript:

Symbol	Description	Units
a	Distance between active sites on the surface	m
A	Attractive interaction constant between molecules or between a molecule and the surface of the material	$J \cdot m^6$
C	Solute concentration in general (may vary across spatial domains)	mol/m^3
$C(r,t)$	Concentration at a radial distance r and time t	mol/m^3
C_v	Solute concentration in the gas phase inside the porous channel	mol/m^3
C_o	Initial solute concentration	mol/m^3

 doi:10.20944/preprints202509.2125.v1

Symbol	Description	Units
d_p	Pore diameter	m
D_{eff}	Effective diffusion coefficient in the porous medium	m²/s
D_v	Diffusion coefficient in the channel volume (combined molecular and Knudsen)	m²/s
D_m	Molecular diffusion coefficient in the free phase (free motion between molecular collisions)	m²/s
D_K	Knudsen diffusion coefficient (dominated by collisions with pore walls)	m²/s
D_s	Surface diffusion coefficient (adsorbate migrating along the pore wall)	m²/s
D_{ij}	Cross-diffusivity coefficient between species i and j	m²/s
D_{oi}	Frictional diffusivity coefficient between species i and the porous solid matrix	m²/s
D_{global}	Overall effective diffusion coefficient in hierarchical materials	m²/s
E_a	Activation energy for surface migration (~5–30 kJ/mol for Van der Waals)	kJ/mol
E_{ads}	Adsorption energy	kJ/mol
$\vec{j}$	Total molar flux vector	mol/(m²·s)
k_a	Adsorption rate constant	1/s
k_d	Desorption rate constant	1/s
l	Interfacial spacing between porous domains (used in hierarchical transport)	m
l_{pp}	Distance between two particles or between an adsorbed molecule and the material surface	m
M	Molar mass of the solute	kg/mol
q_i	Net charge or transport factor of species i	adimensional
r	Radial distance from the pore axis	m
R	Universal gas constant (8.314)	J/mol·K
T	Absolute temperature	K
$\bar{v}$	Average molecular velocity of the solute	m/s
α	Interfacial permeability coefficient in hierarchical transport models	m/s
λ	Mean free path of the molecule	m
ε	Porosity of the medium	dimensionless
τ	Tortuosity of the diffusive path	dimensionless
Γ	Hopping frequency of adsorbate between sites (~10^{12} s^{-1})	1/s
μ_i	Chemical potential of i	dimensionless
θ	Surface coverage fraction (occupied sites over total available)	dimensionless
θ_j	Mole fraction of species j	dimensionless
∇^2	Laplacian operator (gradient of the gradient)	1/m²
∇C	Gradient of concentration field	mol/m⁴
$\nabla \mu_i$	Gradient of chemical potential of species *i*	J/(mol·m)
$\partial/\partial t$	Partial derivative related to time	s^{-1}
$\partial^2/\partial r^2$	Second partial derivative related to the radial coordinate	1/m²

References

1. D. H. Everett, "Manual of Symbols and Terminology for Physicochemical Quantities and Units, Appendix II: Definitions, Terminology and Symbols in Colloid and Surface Chemistry," *Pure and Applied Chemistry*, vol. 31, no. 4, pp. 577–638, May 1972, doi: 10.1351/PAC197231040577.
2. C. T. Kresge, M. E. Leonowizc, W. J. Roth, J. C. Vartuli, and J. S. Beck, "Ordered mesoporous molecular sieves synthesised by a liquid-crystal template mechanism," vol. 359, pp. 710–712, Oct. 1992, doi: https://doi.org/10.1038/359710a0.
3. Y. Wan and D. Zhao, "On the controllable soft-templating approach to mesoporous silicates," Jul. 2007. doi: 10.1021/cr068020s.
4. T. Asefa and V. Dubovoy, "Ordered Mesoporous/Nanoporous Inorganic Materials via Self-Assembly," in *Comprehensive Supramolecular Chemistry II*, vol. 9, Elsevier Inc., 2017, pp. 158–192. doi: 10.1016/B978-0-12-409547-2.12649-6.

 doi:10.20944/preprints202509.2125.v1

5. M. Shakeri, Z. K. Shal, and P. Van Der Voort, "An overview of the challenges and progress of synthesis, characterization and applications of plugged sba-15 materials for heterogeneous catalysis," Sep. 01, 2021, *MDPI*. doi: 10.3390/ma14175082.
6. S. Yuan, M. Wang, J. Liu, and B. Guo, "Recent advances of SBA-15-based composites as the heterogeneous catalysts in water decontamination: A mini-review," Jan. 15, 2020, *Academic Press*. doi: 10.1016/j.jenvman.2019.109787.
7. R. Janus, M. Wądrzyk, M. Lewandowski, P. Natkański, P. Łątka, and P. Kuśtrowski, "Understanding porous structure of SBA-15 upon pseudomorphic transformation into MCM-41: Non-direct investigation by carbon replication," *Journal of Industrial and Engineering Chemistry*, vol. 92, pp. 131–144, Dec. 2020, doi: 10.1016/j.jiec.2020.08.032.
8. J. Asensio, M. I. Beltrán, N. Juáresz-Serrano, and D. Berenguer, "Study of the Decomposition of N-Nitrosonornicotine (NNN)under Inert and Oxidative Atmospheres: Effect of the Additionof SBA-15 and MCM-41," *Applied Sciences*, vol. 12, no. 19, p. 9426, Sep. 2022, doi: https://doi.org/10.3390/app12199426.
9. N. Juárez-Serrano, J. Asensio, I. Blasco, Beltrán Maribel, and A. Marcilla, "Effect of Time, Temperature and Stirring Rate Used in the FirstStep of the Synthesis of SBA-15 on Its Application as Reductorof Tars in Tobacco Smoke," *Catalysis*, vol. 11, no. 3, p. 375, Mar. 2021, doi: https://doi.org/10.3390/catal11030375.
10. A. Sayari and Y. Belmabkhout, "Stabilization of amine-containing CO2 adsorbents: Dramatic effect of water vapor," *J Am Chem Soc*, vol. 132, no. 18, pp. 6312–6314, May 2010, doi: 10.1021/ja1013773.
11. M. Vallet-Regí, M. Colilla, I. Izquierdo-Barba, and M. Manzano, "Mesoporous silica nanoparticles for drug delivery: Current insights," 2018, *MDPI AG*. doi: 10.3390/molecules23010047.
12. Z. Ezzeddine, I. Batonneau-Gener, G. Ghssein, and Y. Pouilloux, "Recent Advances in Heavy Metal Adsorption via Organically Modified Mesoporous Silica: A Review," Mar. 01, 2025, *Multidisciplinary Digital Publishing Institute (MDPI)*. doi: 10.3390/w17050669.
13. P. N. E. Diagboya and E. D. Dikio, "Silica-based mesoporous materials; emerging designer adsorbents for aqueous pollutants removal and water treatment," Aug. 01, 2018, *Elsevier B.V.* doi: 10.1016/j.micromeso.2018.03.008.
14. A. Galarneau, H. Cambon, F. Di Renzo, and F. Fajula, "True microporosity and surface area of mesoporous SBA-15 silicas as a function of synthesis temperature," *Langmuir*, vol. 17, no. 26, pp. 8328–8335, Dec. 2001, doi: 10.1021/la0105477.
15. F. Tang, L. Li, and D. Chen, "Mesoporous silica nanoparticles: Synthesis, biocompatibility and drug delivery," *Advanced Materials*, vol. 24, no. 12, pp. 1504–1534, Mar. 2012, doi: 10.1002/adma.201104763.
16. L. Wang and R. T. Yang, "Increasing selective CO2 adsorption on amine-grafted SBA-15 by increasing silanol density," *Journal of Physical Chemistry C*, vol. 115, no. 43, pp. 21264–21272, Nov. 2011, doi: 10.1021/jp206976d.
17. K. Lan and D. Zhao, "Functional Ordered Mesoporous Materials: Present and Future," Apr. 27, 2022, *American Chemical Society*. doi: 10.1021/acs.nanolett.2c00902.
18. D. Zhao, Q. Huo, J. Feng, B. F. Chmelka, and G. D. Stucky, "Nonionic Triblock and Star Diblock Copolymer and Oligomeric Surfactant Syntheses of Highly Ordered, Hydrothermally Stable, Mesoporous Silica Structures," 1998.
19. N. Juárez-Serrano, D. Berenguer, I. Martínez-Castellanos, I. Blasco, M. Beltrán, and A. Marcilla, "Effect of reaction time and hydrothermal treatment time on the textural properties of sba-15 synthesized using sodium silicate as a silica source and its efficiency for reducing tobacco smoke toxicity," *Catalysts*, vol. 11, no. 7, Jul. 2021, doi: 10.3390/catal11070808.
20. N. Rahmat, A. Z. Abdullah, and A. R. Mohamed, "A review: Mesoporous Santa Barbara amorphous-15, types, synthesis and its applications towards biorefinery production," 2010, *Science Publications*. doi: 10.3844/ajassp.2010.1579.1586.
21. M. Pérez-Page *et al.*, "Template-based syntheses for shape controlled nanostructures," Aug. 01, 2016, *Elsevier B.V.* doi: 10.1016/j.cis.2016.04.001.
22. [22] A. Tewodros, Mark J. MacLachlan, Neil Coombs, and Geoffrey A. Ozin, "Periodic mesoporous organosilicas with organic groups inside the channel wall," vol. 402, pp. 867–871, Dec. 1999, doi: https://doi.org/10.1038/47229.

 doi:10.20944/preprints202509.2125.v1

23. T. Asefa and V. Dubovoy, "Ordered Mesoporous/Nanoporous Inorganic Materials via Self-Assembly," in *Comprehensive Supramolecular Chemistry II*, vol. 9, Elsevier Inc., 2017, pp. 158–192. doi: 10.1016/B978-0-12-409547-2.12649-6.
24. D. Zhao *et al.*, "Triblock Copolymer Syntheses of Mesoporous Silica with Periodic 50 to 300 Angstrom Pores," *Science (1979)*, vol. 279, no. 5350, p. 548, Jan. 1998, doi: 10.1126/science.279.5350.548.
25. E. Serra, R. M. Blanco, and I. Díaz, "Síntesis y caracterización de materiales mesoporosos ordenados y su aplicación como soportes en la inmovilización de lipasa," *An. Quím*, vol. 104, no. 2, pp. 97–103, 2008, [Online]. Available: www.rseq.org
26. W. Han, Y. Jia, G. Xiong, and W. Yang, "Template-free sol-gel synthesis of mesoporous materials with ZSM-5 structure walls," in *Studies in Surface Science and Catalysis*, vol. 165, Elsevier Inc., 2007, pp. 515–518. doi: 10.1016/S0167-2991(07)80373-9.
27. Y. G. Asfaha, A. K. Tekile, and F. Zewge, "Hybrid process of electrocoagulation and electrooxidation system for wastewater treatment: A review," Oct. 01, 2021, *Elsevier Ltd*. doi: 10.1016/j.clet.2021.100261.
28. J. Zhao and W. Yan, "Microwave-assisted Inorganic Syntheses," in *Modern Inorganic Synthetic Chemistry*, Elsevier, 2011, pp. 173–195. doi: 10.1016/B978-0-444-53599-3.10008-3.
29. C. P. Avanzadas and P. V. Vigón, "Síntesis de materiales mesoporosos compuestos sílice/cabono y su empleo como plataforma para la fabricación de materiales," 2013.
30. J. García Martínez, "Sólidos ordenados desde la nano a la macroestructura," *An. Quim*, 2006, [Online]. Available: www.rseq.org
31. J. H. Williams, Q. Zheng, M. D. Mantle, A. J. Sederman, and L. F. Gladden, "Probing the Diffusion Mechanism of n-Alkanes in Mesoporous Confinement Using Pulsed Field Gradient NMR," *Journal of Physical Chemistry C*, vol. 127, no. 31, pp. 15326–15335, Aug. 2023, doi: 10.1021/acs.jpcc.3c02793.
32. P. Kumar and V. V. Guliants, "Periodic mesoporous organic-inorganic hybrid materials: Applications in membrane separations and adsorption," Jul. 2010. doi: 10.1016/j.micromeso.2010.02.007.
33. L. Zheng, Y. Yang, Y. Zhang, T. Zhu, and X. Wang, "Functionalization of SBA-15 mesoporous silica with bis-schiff base for the selective removal of Pb(II) from water," *J Solid State Chem*, vol. 301, Sep. 2021, doi: 10.1016/j.jssc.2021.122320.
34. D. Li *et al.*, "β-Cyclodextrin functionalized SBA-15 via amide linkage as a super adsorbent for rapid removal of methyl blue," *J Colloid Interface Sci*, vol. 583, pp. 100–112, Feb. 2021, doi: 10.1016/j.jcis.2020.09.006.
35. L. Xiang Chuin, S. Kamaruzaman, S. Mangala Praveena, and N. Yahaya, "Recent applications of β-cyclodextrin in selective adsorption of Pesticides, heavy metals, and organic pollutants from water Samples: Mini review," *Microchemical Journal*, p. 111583, Nov. 2024, doi: 10.1016/j.microc.2024.111583.
36. F. das C. M. da Silva, M. J. dos S. Costa, L. K. R. da Silva, A. M. Batista, and G. E. da Luz, "Functionalization methods of SBA-15 mesoporous molecular sieve: a brief overview," Jun. 01, 2019, *Springer Nature*. doi: 10.1007/s42452-019-0677-z.
37. D. Shimon *et al.*, "15N Solid State NMR Spectroscopic Study of Surface Amine Groups for Carbon Capture: 3-Aminopropylsilyl Grafted to SBA-15 Mesoporous Silica," *Environ Sci Technol*, vol. 52, no. 3, pp. 1488–1495, Feb. 2018, doi: 10.1021/acs.est.7b04555.
38. R. Ojeda-López, I. J. Pérez-Hermosillo, J. Marcos Esparza-Schulz, A. Cervantes-Uribe, and A. Domínguez-Ortiz, "SBA-15 materials: calcination temperature influence on textural properties and total silanol ratio," *Adsorption*, vol. 21, no. 8, pp. 659–669, Nov. 2015, doi: 10.1007/s10450-015-9716-2.
39. Z. Zhang, J. Yin, H. J. Heeres, and I. Melián-Cabrera, "Thermal detemplation of SBA-15 mesophases. Effect of the activation protocol on the framework contraction," *Microporous and Mesoporous Materials*, vol. 176, pp. 103–111, 2013, doi: 10.1016/j.micromeso.2013.03.048.
40. Á. Szegedi, K. Lázár, H. Solt, and M. Popova, "Peculiar redox properties of SBA-15 supported copper ferrite catalysts promoting total oxidation of a model volatile organic air pollutant," *Surfaces and Interfaces*, vol. 56, Jan. 2025, doi: 10.1016/j.surfin.2024.105498.
41. A. Gouveia Gil, Z. Wu, D. Chadwick, and K. Li, "Ni/SBA-15 Catalysts for combined steam methane reforming and water gas shift - Prepared for use in catalytic membrane reactors," *Appl Catal A Gen*, vol. 506, pp. 188–196, Oct. 2015, doi: 10.1016/j.apcata.2015.09.009.

42. Ł. Laskowski *et al.*, "Mesoporous silica SBA-15 functionalized by nickel-phosphonic units: Raman and magnetic analysis," *Microporous and Mesoporous Materials*, vol. 200, pp. 253–259, Jul. 2014, doi: 10.1016/j.micromeso.2014.08.041.
43. H. Wu, Y. Xiao, Y. Guo, S. Miao, Q. Chen, and Z. Chen, "Functionalization of SBA-15 mesoporous materials with 2-acetylthiophene for adsorption of Cr(III) ions," *Microporous and Mesoporous Materials*, vol. 292, Jan. 2020, doi: 10.1016/j.micromeso.2019.109754.
44. X. Xia, Y. Jin, H. Zhao, G. Wang, and D. Huang, "Optimization and Experiment of Hot Air Drying Process of Cyperus esculentus Seeds," *Agriculture (Switzerland)*, vol. 13, no. 3, Mar. 2023, doi: 10.3390/agriculture13030617.
45. Y. Wang and R. T. Yang, "Template Removal from SBA-15 by Ionic Liquid for Amine Grafting: Applications to CO2Capture and Natural Gas Desulfurization," *ACS Sustain Chem Eng*, vol. 8, no. 22, pp. 8295–8304, Jun. 2020, doi: 10.1021/acssuschemeng.0c01941.
46. F. Hoffmann, M. Cornelius, J. Morell, and M. Fröba, "Silica-based mesoporous organic-inorganic hybrid materials," *Angewandte Chemie - International Edition*, vol. 45, no. 20, pp. 3216–3251, May 2006, doi: 10.1002/anie.200503075.
47. Y. Yin *et al.*, "Modification of as Synthesized SBA-15 with Pt nanoparticles: Nanoconfinement Effects Give a Boost for Hydrogen Storage at Room Temperature," *Sci Rep*, vol. 7, no. 1, Dec. 2017, doi: 10.1038/s41598-017-04346-9.
48. J. Zhu, T. Wang, X. Xu, P. Xiao, and J. Li, "Pt nanoparticles supported on SBA-15: Synthesis, characterization and applications in heterogeneous catalysis," Feb. 07, 2013. doi: 10.1016/j.apcatb.2012.11.005.
49. A. Taguchi and F. Schüth, "Ordered mesoporous materials in catalysis," in *Microporous and Mesoporous Materials*, vol. 77, no. 1, 2005, pp. 1–45. doi: 10.1016/j.micromeso.2004.06.030.
50. Ł. Laskowski *et al.*, "Mesoporous silica SBA-15 functionalized by nickel-phosphonic units: Raman and magnetic analysis," *Microporous and Mesoporous Materials*, vol. 200, pp. 253–259, Jul. 2014, doi: 10.1016/j.micromeso.2014.08.041.
51. F. das C. M. da Silva, M. J. dos S. Costa, L. K. R. da Silva, A. M. Batista, and G. E. da Luz, "Functionalization methods of SBA-15 mesoporous molecular sieve: a brief overview," Jun. 01, 2019, *Springer Nature*. doi: 10.1007/s42452-019-0677-z.
52. J. Kärger and D. M. Ruthven, "Diffusion in nanoporous materials: Fundamental principles, insights and challenges," 2016, *Royal Society of Chemistry*. doi: 10.1039/c5nj02836a.
53. W. Li, J. Liu, and D. Zhao, "Mesoporous materials for energy conversion and storage devices," May 04, 2016, *Nature Publishing Group*. doi: 10.1038/natrevmats.2016.23.
54. J. Kärger and R. Valiullin, "Mass transfer in mesoporous materials: The benefit of microscopic diffusion measurement," *Chem Soc Rev*, vol. 42, no. 9, pp. 4172–4197, Apr. 2013, doi: 10.1039/c3cs35326e.
55. S. Whitaker, *The Method of Volume Averaging*, vol. 13. in Theory and Applications of Transport in Porous Media, vol. 13. Dordrecht: Springer Netherlands, 1999. doi: 10.1007/978-94-017-3389-2.
56. R. B. Bird, S. W. Earl, and E. N. Lightfoot, *Fenómenos de Transporte*, 2nd ed. 2010. [Online]. Available: https://books.google.com/books/about/Transport_Phenomena.html?id=L5FnNlIaGfcC
57. J. Kärger, D. Freude, and J. Haase, "Diffusion in nanoporous materials: Novel insights by combining MAS and PFG NMR," Sep. 01, 2018, *MDPI AG*. doi: 10.3390/pr6090147.
58. A. Zhokh, "Size-controlled non-Fickian diffusion in a combined micro- and mesoporous material," *Chem Phys*, vol. 520, pp. 27–31, Apr. 2019, doi: 10.1016/j.chemphys.2018.12.013.
59. D. Do. Duong, Adsorption analysis: equilibria and kinetics, vol. 1. Imperial College Press, 1998.
60. V. T. Hoang, Q. Huang, M. Eić, T. O. Do, and S. Kaliaguine, "Structure and diffusion characterization of SBA-15 materials," *Langmuir*, vol. 21, no. 5, pp. 2051–2057, Mar. 2005, doi: 10.1021/la048349d.
61. H. Rusinque and G. Brenner, "Mass transport in porous media at the micro- and nanoscale: A novel method to model hindered diffusion," *Microporous and Mesoporous Materials*, vol. 280, pp. 157–165, May 2019, doi: 10.1016/j.micromeso.2019.01.037.
62. J. Kärger and D. M. Ruthven, "Diffusion in nanoporous materials: Fundamental principles, insights and challenges," 2016, *Royal Society of Chemistry*. doi: 10.1039/c5nj02836a.

 doi:10.20944/preprints202509.2125.v1

63. S. Whitaker, *The Method of Volume Averaging*, vol. 13. in Theory and Applications of Transport in Porous Media, vol. 13. Dordrecht: Springer Netherlands, 1999. doi: 10.1007/978-94-017-3389-2.
64. A. Vignes, "Diffusion in Binary Solutions Variation of Diffusion Cocficient with Compositionsion," *Ind. Eng. Chem. Fundam*, vol. 5, no. 2, pp. 189–199, 1966, doi: https://doi.org/10.1021/i160018a007.
65. G. Guevara-Carrion, T. Janzen, Y. M. Muñoz-Muñoz, and J. Vrabec, "Mutual diffusion of binary liquid mixtures containing methanol, ethanol, acetone, benzene, cyclohexane, toluene, and carbon tetrachloride," *Journal of Chemical Physics*, vol. 144, no. 12, Mar. 2016, doi: 10.1063/1.4943395.
66. J. N. Israelachvili, "Intermolecular and Surface Forces: Third Edition," in *Intermolecular and Surface Forces: Third Edition*, 3thd ed., Elsevier Inc., 2011, pp. 1–676. doi: 10.1016/C2011-0-05119-0.
67. Javier. García-Martínez and Elena. Serrano-Torregrosa, *Chemistry Education : Best Practices, Opportunities and Trends*. Wiley, 2015.
68. A. Larki, S. J. Saghanezhad, and M. Ghomi, "Recent advances of functionalized SBA-15 in the separation/preconcentration of various analytes: A review," Oct. 01, 2021, *Elsevier Inc.* doi: 10.1016/j.microc.2021.106601.
69. N. Linares, A. M. Silvestre-Albero, E. Serrano, J. Silvestre-Albero, and J. García-Martínez, "Mesoporous materials for clean energy technologies," Nov. 21, 2014, *Royal Society of Chemistry*. doi: 10.1039/c3cs60435g.